EUR 3736 e

EUROPEAN ATOMIC ENERGY COMMUNITY - EURATOM

SPECTRUM INDICES MEASUREMENTS IN ORGEL TYPE UC CLUSTER FUEL ELEMENTS

by

F. CONTI

1968

ORGEL Program

Joint Nuclear Research Center
Ispra Establishment - Italy

Reactor Physics Department
Experimental Neutron Physics

LEGAL NOTICE

This report is on sale at the addresses listed on cover page 4

at the price of FF 6.—	FB 60.—	DM 4.80	Lir. 750	Fl. 4.30

When ordering, please quote the EUR number and the title, which are indicated on the cover of each report.

Printed by Guyot, s.a.
Brussels, January 1968

EUR 3736 e

SPECTRUM INDICES MEASUREMENTS IN ORGEL TYPE UC CLUSTER FUEL ELEMENTS by F. CONTI

European Atomic Energy Community - EURATOM
ORGEL Program
Joint Nuclear Research Center - Ispra Establishment (Italy)
Reactor Physics Department - Experimental Neutron Physics
Brussels, January 1968 - 40 Pages - 16 Figures - FB 60

Results of index spectrum measurements performed in natural uranium carbide cluster type fuel elements are described. Both the epithermal and the thermal spectrum indices were determined by means of integral activation techniques, using foil detectors with resonances, respectively in the epithermal and maxwellian regions. The resonance activities are normalized to that of a 1/v detector. The activity ratios are interpreted with the aid of the Westcott's convention.

EUR 3736 e

SPECTRUM INDICES MEASUREMENTS IN ORGEL TYPE UC CLUSTER FUEL ELEMENTS by F. CONTI

European Atomic Energy Community - EURATOM
ORGEL Program
Joint Nuclear Research Center - Ispra Establishment (Italy)
Reactor Physics Department - Experimental Neutron Physics
Brussels, January 1968 - 40 Pages - 16 Figures - FB 60

Results of index spectrum measurements performed in natural uranium carbide cluster type fuel elements are described. Both the epithermal and the thermal spectrum indices were determined by means of integral activation techniques, using foil detectors with resonances, respectively in the epithermal and maxwellian regions. The resonance activities are normalized to that of a 1/v detector. The activity ratios are interpreted with the aid of the Westcott's convention.

EUR 3736 e

EUROPEAN ATOMIC ENERGY COMMUNITY - EURATOM

SPECTRUM INDICES MEASUREMENTS IN ORGEL TYPE UC CLUSTER FUEL ELEMENTS

by

F. CONTI

1968

ORGEL Program

Joint Nuclear Research Center
Ispra Establishment - Italy

Reactor Physics Department
Experimental Neutron Physics

SUMMARY

Results of index spectrum measurements performed in natural uranium carbide cluster type fuel elements are described. Both the epithermal and the thermal spectrum indices were determined by means of integral activation techniques, using foil detectors with resonances, respectively in the epithermal and maxwellian regions. The resonance activities are normalized to that of a 1/v detector. The activity ratios are interpreted with the aid of the Westcott's convention.

KEYWORDS

FUEL ELEMENT CLUSTERS
ORGEL REACTOR
URANIUM CARBIDES
SPECTRA
NEUTRONS
THERMAL NEUTRONS
EPITHERMAL NEUTRONS
ACTIVATION
FOILS
WESTCOTT CROSS SECTIONS

SPECTRUM INDICES MEASUREMENTS IN ORGEL TYPE UC CLUSTER FUEL ELEMENTS(+)

1. Introduction

The activation techniques give only integral information and the total neutron density. The differential distribution n(v) is not a priori known. But with reasonable assumptions on the distribution some parameters are obtainable directly from foils activation data (Ref.1,2) defining the neutron spectrum.

At present three widely known procedures for epithermal spectrum index measurements are used, i.e. the Cd ratio, the sandwich and the two foils method. All these techniques utilise resonance detectors.

With the cadmium ratio method, the activity of a Cd-shielded detector is normalized on the activity of the bare detector irradiated in the same neutron flux. The Cd ratio method has the advantage that only one detector type for the epithermal index is needed. This means the same measuring technique, counter efficiency, reference cross sections are useable. The use of the cadmium ratio method was abandoned due to the large perturbation of the neutron fluxes and the poor spatial resolution.

In the "sandwich" method (Ref.3) detectors with a single, sharp resonance are irradiated bare and in a sandwich of three in the same flux. The difference between the activities of the bare foil and the sandwich central foil is proportional to the neutron density at the detector resonance energy. This method has the disadvantage that a reference spectrum with an epithermal component is required. As no reference calibration spectrum with epithermal component was available this method could not be applied.

(+) Manuscript received on July 7, 1967.

In the two foil method the activity of a resonance detector is normalized to the activity of a detector with a 1/v activation cross section. In the Westcott convention the factors g and s are then 1 and 0 respectively. Calibration runs of the two detectors in a known thermal reference spectrum are preferred to cancel out in the activity ratios the counter efficiencies, the normalized cross sections, and time corrections. This method was used to characterize the thermal and epithermal spectrum.

2. Theory of the Experiment

In the two foil method, the ratio of the normalized activity of a detector A to the activity of a detector B is performed

$$R_{A-B} = \frac{\int_0^\infty \sigma_{a_A}(E)\,\phi_u(E)\,G_A(E)\,dE}{\int_0^\infty \sigma_{a_B}(E)\,\phi_u(E)\,G_B(E)\,dE} \cdot \frac{\int_0^\infty \sigma_{a_B}\,\phi_m(E)\,G_B(E)\,dE}{\int_0^\infty \sigma_{a_A}\,\phi_m(E)\,G_A(E)\,dE} \qquad (1)$$

with

$\phi_u(E)$ = differential neutron flux in an unknown spectrum
$\phi_m(E)$ = differential neutron flux of a maxwellian distribution
$\sigma_a(E)$ = activation (or fission) cross section at energy E
$G(E)$ = flux depression factor of the foil at energy E

This ratio depends only on the spectrum dependant foil self shielding factors.

With the Westcott's convention (Ref.2,4) equ.(2) becomes:

$$R_{A-B} = \frac{g_A(T)\,G_{th\,A}(T) + r\,s_A(T)\,G_{r,A}(T)}{g_B(T)\,G_{th\,B}(T) + r\,s_B(T)\,G_{r\,B}(T)} \quad \frac{g_B(T_M)\,G_{th\,B}(T_M)}{g_A(T_M)\,G_{th\,A}(T_M)} \qquad (2)$$

$g(T)$, $s(T)$	= Westcott's factors
r	= epithermal fraction of neutron population
G_{th}, G_r	= maxwellian and epithermal self shielding factors
T	= neutron temperature in unknown spectrum
T_M	= neutron temperature of maxwellian reference spectrum

If the element B has a 1/v cross section at least in the maxwellian region, it is:

$$R_{A-B} = \frac{g_A(T)\,G_{th\,A}(T) + r'\sqrt{\frac{T_o}{T}}\,s_A(T)\,G_{r\,A}(T)}{G_{th\,B}(T) + r'\,s_{o\,B}} \quad \frac{G_{th.B}(T_M)}{g_A(T_M)\,G_{th\,A}(T_M)} \qquad (3)$$

with

$$r' = r\sqrt{T/T_o} \qquad (4)$$

T_o is the reference temperature, taken equal to the physical temperature.

The expression

$$s(T) = s_o\sqrt{T/T_o} \qquad (5)$$

holds for all elements with the first resonance sufficiently above the thermal region.

The detectors used were the couples Lu-Mn for thermal spectrum index (i.e. neutron temperature,T) and In-Mn or Au-Mn for the epithermal index r. Actually, the Westcott assumptions in the fuel break down because of the strong absorption in the U^{238} resonance region and in the thermal range. The gold with its resonance energy at 4.906 eV, cannot be utilized in the fuel, because its resonance is influenced by those of the U^{238}. Gold was used in the moderator only. The lutetium is particularly useful as thermal indicator because of its resonance cross section of σ_r = 13630 b at E_r = 0,142 eV (Ref.5). As 1/v detector the Mn^{55} has been chosen although a small high energy (377 eV) resonance implies a small correction.

The spectrum indices are obtained solving the system:

$$\begin{cases} R_{In-Mn} = f_1(T, r) \\ R_{Lu-Mn} = f_2(T, r) \\ r = r' \sqrt{T_o / T} \end{cases} \qquad (6)$$

where f_1 and f_2 are functions of the type indicated at the right side of e quation (3).

The R_{Lu-Mn} must be corrected if the thermal spectrum irradiation is carried out at a temperature T_M different from the physical temperature T_o in the unknown spectrum position. This can be easily done with the following relation using Westcott's "g" factors:

$$(R_{Lu-Mn})_{corrected} = (R_{Lu-Mn})_{uncorr.} \frac{g_{Lu}(T_M)}{g_{Lu}(T_o)} \qquad (7)$$

3. Experimental Arrangement

The measurement were performed utilizing the ECO reactor (Ref.6) with two different ORGEL type uranium carbide cluster elements. A brief description of the fuel elements, the detector materials, the irradiation conditions and the counting technique is given.

3.1 Investigated lattices

The irradiations had been carried out with the ECO reactor core loaded with a driver zone composed of natural uranium metal U/19/12 (ECO reference) fuel elements, and with a central test zone of twenty one UC/4/30.9 or thirteen UC/7/25.2 fuel elements. In the central cell of the test zone existed the same neutron spectrum of a reactor completely loaded with such fuel elements. The dimensions of the tested elements are given in table 1 and cross sectional views in figures 1 and 2 .
Measurements were performed with the elements UC/4/30.9 at the pitches 18.80 - 23.50 - 28.05 cm and with elements UC/7/25.2 at pitch 28.05 cm only.

3.2 Activation detectors and their arrangement.

All detectors are aluminium alloyed foils, prepared in the Euratom center of Geel, Belgium, following the techniques described in (Ref. 7). The properties of the foils are given in tables 2 and 3. Since the self-shielding factors are spectrum dependent, very thin detectors were used.

Table 1: Characteristics of UC clustered fuel elements investigated.

number of rods in the cluster	diameter of rods (mm)	rod cladding (Al)		pressure tube (Al)		calandria tube (Al)		spacing between rods (mm)	coolant	observations
		Øint (mm)	Øext (mm)	Øint (mm)	Øext (mm)	Øint (mm)	Øext (mm)			
4	30.9	31.1	33.2	38.2	39.2	110	114	3.8	air	with graphit matrix
7	25.2	23.4	27.2	91.0	95.0	101	104	2.3	diphyl	-

Table 2: Physical specifications of the foil material.

detector material	indium	manganese	lutetium	gold
isotope used	115	55	176	197
isotope natural abundance	95.72%	100%	2.59%	100%
density(g/cm^3)	7.28	7.30	9.74	19.32
density($atoms/cm^3$)	$3.82.10^{22}$	$7.89.10^{22}$	$3.35.10^{22}$	$5.91.10^{22}$
microscopic absorption cross section $\sigma_a(2200)$	160b$\pm$2	13.2b	2073.3b	98.7b
macroscopic absorption cross section $\Sigma_a(2200)$	$5.89cm^{-1}$	$1.04cm^{-1}$	$134cm^{-1}$	$5.79cm^{-1}$
main resonance energies (eV)	1.457 3.86	1/v cross section	0.142 1.57	4.906
resonance peak cross section σ_r	2.810b 43.5b		13.630b	32.900b
half life $T_{\frac{1}{2}}$	54.14min	223.32min	6.72days	2.7days
decay constant	$2.1337.10^{-4}$ s^{-1}	$7.4722.10^{-5}$ s^{-1}	$1.1806.10^{-6}$ s^{-1}	$2.9744.10^{-6}$ s^{-1}
Westcott's g(20°C)	1.019	1.0	strongly temperature	1.005
parameters S_4(20°C)	18.80$\pm$0.4	0.814	dependent	17.0$\pm$0.5

Table 3: Specifications of the foils used.

detector materials	indium		manganese		lutetium		gold
content%	0.200±0.004		1.46±0.02%		5.92±0.06%		0.372±0.005%
analysis accuracy	±1.0%		±1.3%		-		±1.5%
foil thickness(mm)	0.5		0.5		0.5		0.5
detector equivalent thickness(mg/cm^2)	0.265(0.250 In^{115})		1.96		8.29(0.215Lu^{176})		0.502
" (cm)	$3.65.10^{-5}$($3.50.10^{-5}$)		$2.70.10^{-4}$		$8.31.10^{-4}$($2.20.10^{-5}$)		$2.61.10^{-5}$
foil diameter (mm)	6.00	25.20	6.00	25.20	6.00	25.20	6.00
average foil weight(mg)	37.5	665.0	37.5	665.0	39.6	369.0	38.1
detector preparation techniques	induction melting		levitation melting		levitation melting		levitation melting

The measurements (or irradiations) were performed inside a special designed fuel element. It has 2 or 3 removable rods (depending on the type of the cluster), each composed of 3 segments with 30 cm length. Figures 3 and 4 show a removable rod and the special fuel element, respectively.

Each segment consists of precisely machined UC pellets canned in an aluminium tube with leak proof seals. A special design of the upper and lower rod supporting heads allow a fast dismounting.

In the case of the UC/4/30.9 rod cluster 6.00 mm diameter, 0.5mm thick detectors were choosen. In the UC/7/25.2 only integral measurements had been performed using disks of 25.2 mm diameter and 0.5 mm thick. In the first case the detectors were housed inside special pellets (fig. 5). In the 25.2 mm rods the disks were sandwiched between 2 consecutive pellets. In order to get the highest activation and to minimize gradient effects the detectors were placed in the center of the central segment of the special fuel element in the maximum flux region. All detectors in fuel and moderator were aligned along a diameter at the same height (fig. 6). An axial slot in the aluminium cladding fitting into the pellets prevents any pellet rotation.(fig.5)

The detectors were protected against fission product contaminations by 40 microns thick aluminium catchers. The detectors in the moderator were fixed on 50 microns thick mylar films supported by 2 small Al rods on which spacers ascertain the radial film position (fig. 7). The whole device is suspended to a supported thimble. This device allowed the insertion of the detector support into the reactor and an optimum D_2O surrounding for the foils.

3.3 Irradiation conditions

The irradiations in ECO reactor were performed at a neutron flux of ca. 5.10^7 n/cm^2s. Since in ECO exists no thermal reference positions, the irradiated foils had been previously calibrated in the Ispra-I reactor thermal column. During the reference irradiation the detectors were stuck on a rotating disk to cancel out local flux differences. For every run the irradiation times (120 min) and cooling down times were kept the same to minimize timing errors. The activations during the start-up and shut down transients were taken into account. The physical temperatures both in ECO and in the thermal column were recorded. The applied temperature corrections of relationship (7) were in any case below 2 percents.

3.4 Counting Techniques

Due to the fact that simultaneous irradiations in ECO and in the thermal reference spectrum were not possible, much care has been devoted to the counting chain stability and reproducability of counting conditions.

A two channel- -counting chain selected for high short term stability was used for counting. Several foils could be counted consecutively without a necessary drift correction.

The gain stability was checked periodically with Cs137 standard source. The two flankes of the 0.661 MeV Cs peak were counted with the windows of two single channel analysers. The ratio of the counts in the two channels is plotted as a function of gain and photomultiplier high tension (Fig.8). Entering the curve with the measured

ratio C_1/C_2 the correction on the high voltage is obtained in order to readjust the overall gain to its nominal value.

This is a very sensitive drift detecting method since 1% overall gain drift corresponds to ca. 40% count ratio variation.

The counting procedure adopted for the different detector types is shown in table 4.

Table 4. Counting modes of the used detectors.

detector type	main resonance energy-peaks (MeV)	counting mode	threshold setting (MeV)
In^{115}	0.406-0.82-1.085 1.274-1.487-2.090	integral	0.36
Mn^{55}	0.85-1.81-2.13	differential	0.715-0.922
Lu^{176}	0.055-0.113-0.208 0.250-0.321	integral	0.037
Au^{198}	0.411	differential	0.350-0.452

All data were elaborated on IBM 7090 computer, corrected for dead time, background and decay. The program used for this aim (Ref.8) computes weighted averages, saturation activities, standard deviations and applies statistical tests for data rejection.

4. Experimental Results and Discussion

4.1 Activity ratios

All experimental activity ratios are collected in the table 5 and 6 and plotted as a function of the distance from the cluster center in the figures 9, 10 and 11. The activity ratios increase going from the moderator into the fuel and with increasing fuel to moderator ratio. Inside the fuel pencils of the UC/4/30.9 cluster the reaction rates show the expected maximum. Inside the pencils of the UC/7/25.2 cluster only average activity ratios were measured. At a distance of about 3,5 cm from the surface of the calandria tube the activity ratios in the moderator are constant within the limits of the experimental errors.

The activity ratios derived from In-Mn and Au-Mn agree well with each other in the moderator in regions far from the fuel (Fig.11). Near the fuel element the Au-Mn activity ratio becomes smaller than the In-Mn ratio due to the flux depression caused by the U238 resonances just above the Au resonance energy.

All activity ratios are affected by random and systematic errors. The different error sources are listed in table 7 and the individual values quoted refer to a typical irradiation in an unknown spectrum. The errors of the thermal spectrum reference calibration are smaller and in the order of 0.75%.

Table 5

UC/4/30.9 Activation rate ratios values

distance from core center		15.0	20.5	25.5	30.5	35.5	40.5	46.0	caland. tube 57	cell bound.
pitch 18.0 cm	$R_{In,Mn}$	2.79	2.88	2.92	2.86	2.72	2.57	2.34	2.08	1.81
	$R_{Au,Mn}$								2.04	1.81
	$R_{Lu,Mn}$	1.22	1.23	1.24	1.23	1.21	1.18	1.14	1.09	1.03
pitch 23.05 cm	$R_{In,Mn}$	2.10	2.17	2.20	2.17	2.08	1.94	1.83	1.63	1.50
	$R_{Au,Mn}$								1.61	1.52
	$R_{Lu,Mn}$	1.20	1.22	1.23	1.22	1.19	1.17	1.13	1.06	1.02
pitch 23.05 cm	$R_{In,Mn}$	1.75	1.80	1.85	1.79	1.72	1.67	1.53	1.44	1.29
	$R_{Au,Mn}$								1.40	1.30
	$R_{Lu,Mn}$	1.18	1.20	1.21	1.21	1.18	1.14	1.10	1.0	1.01

Table 6

UC/7/25.2 Activation rate ratios values

detector positions		center rod	outer rod	cluster average	caland. tube 54	64	89	133	cell bound. 188
pitch 28.05 cm	$R_{In,Mn}$	2.10	1.73	1.78	1.37	1.34	1.30	1.27	1.25
	$R_{Au,Mn}$				1.33	1.31	1.29	1.26	1.25
	$R_{Lu,Mn}$	1.29	1.23	1.235	1.07	1.02	1.02	1.01	1.09

Table 7 : Relative Errors of the Activity Ratios

Source of errors	Magnitude
1. random errors	
statistical error in counting	0.45%
background effect (only in R_{Lu-Mn})	0.2%
gain drift effects on the counting rate	0.2%
2. systematic errors	
rod rotation effects	0.2%
gradient effect	0.1%
dead time, pile-up, discriminator threshold setting etc.	1.0%
3. thermal column calibration	0.75%

The In, Au and Mn background counts are negligeable with respect to the obtained activities. In the case of Lu a contribution of 0.5 ÷ 2% to the total activity was measured. Before every irradiation every Lu detector had been counted with 10% accuracy, that means a random error due to the background less than 0.2%.

Gain drifts were periodically corrected back and every foil set was counted in direct and inverse sequence to compensate linear time dependent perturbations. Overall gain drift effects can be quoted within 0.2%.

Timing errors and physical temperature variations inside the reactor lead to negligible effects.

Two types of systematic errors affect the activity ratio measurements, namely those deriving from wrong positioning of the detectors in the reactor lattices and those arising from the foil counting procedures.

Big care had been put to avoid reciprocal rotations of the rods with respect to the pressure tube and of this one with respect to the calandria tube. Such errors can be evaluated to 0.2% and 0.8% respectively in the worst case. Wrong positionong of the foils at the cell boundary and rods relative axial displacement of one rod against the others have no effect on the activity ratios. The axial flux gradient may also introduce a 0.1% error due to the particular foil arrangements.

Systematic counting errors may come from dead time uncertainties, pile-up effects and discriminator threshold setting calibrations and are of the order of 1%.

The local flux depression caused by the foils in the moderator is certainly negligeable. Since the detector cross sections are much lower than that of the fuel, local perturbation and streaming effects may have occured in the fuel pencils but it had not been possible to evaluate them properly.

4.2 Spectrum index values

The thermal and epithermal spectrum indices were calculated solving the system (7) with an iterative procedure. Assuming in the zero approximation a value of the neutron temperature equal to the physical temperature, the term $r'=r\sqrt{T/T_o}$ is calculated from measured R_{In-Mn}.

Table 8

UC/4/30.9 Westcott's spectral indices

Distance from core center(mm)		15.0	20.5	25.5	30.5	35.5	40.5	46	cal. tube 57	cell bound.
Pitch 18.8 T_o= 21.9	$r\sqrt{T/T_o}$	.116	.122	.125	.121	.111	.101	.0851	.067	.050
	r	.102	.106	.108	.106	.0985	.091	.079	.0645	.049
	T(°C)	107	113	120	113	102	90.0	70.8	49.1	30.7
Pitch23.50 T_o= 22.2	$r\sqrt{T/T_o}$	.068	.073	.075	.073	.0670	.058	.051	.038	.030
	r	.062	.066	.067	.065	.059	.054	.048	.037	.030
	T(°C)	84.4	91.8	95.5	92.0	86.1	74.7	57.9	37.7	26.5
Pitch 28.05 T_o = 22.6	$r\sqrt{T/T_o}$	.046	.049	.052	.048	.044	.041	.032	.0265	.017
	r	.042	.0445	.047	.044	.040	.038	.031	.026	.017
	T(°C)	76.0	82.3	85.4	83.4	73.4	63.6	49.9	35.0	24.9

Table 9

UC/7/25.2 Westcott's spectral indices

Detector position (mm)		center rod	outer rod	cluster average	cal. tube 54	64	89	133	cell bound. 188
Pitch 28.05cm T_o = 21,9 °C	$r\sqrt{T/T_o}$	.068	.044	.048	.022	.020	.018	.0165	.015
	r	.059	.040	.043	.022	.020	.018	.0165	.015
	T(°C)	114	87.2	91.0	39.6	27.4	26.1	23.2	23.4

With the known r', the function

$$f_2(T,r) = R_{Lu-Mn}$$

is easily computed.

With the experimental value of R_{Lu-Mn} the spectrum indices T and r are directly obtained. This T value is used for the new iteration process.

The spectrum indices are collected in table 8 and 9 and plotted in the figures 12, 13 and 14 as function of the distance from cluster center.

The evaluated neutron temperatures at the cell boundary positions are systematically slightly above the physical temperature. The line of hardest spectrum in the UC/4 cluster element is about 120°C at the smallest measured pitch. The thermal and epithermal indices T and r increase in the fuel more pronounced than in the moderator with decreasing lattice pitch (Fig.15 and 16).

The errors associated to the nuclear data uncertainties and self-shielding factors affect, together with the above quoted experimental errors, the calculated spectral index values.

From equation (3) it is possible to derive the r' value:

$$r' = \frac{R_{x-Mn} - C_1(T,T_M)}{s_{\circ x}\, C_2(T,T_M) - R_{x-Mn}\, s_{\circ Mn}\, C_3(T,T_M)} \qquad (8)$$

where x may be indium or gold.

The error of the spectral index r' is given in equation (9) (Ref.12).

$$\frac{\Delta r'}{r'} = \frac{\Delta R / R}{1 - C_1 / R} + \frac{\Delta s_{0X} / s_{0X}}{1 - R \frac{s_{0Mn} C_3}{s_{0X} C_2}} + \frac{\Delta R/R + \Delta s_{0Mn}/s_{0Mn}}{\frac{s_{0X} C_2}{s_{0Mn} C_3 \cdot R} - 1} \quad (9)$$

Since the self-shielding and Westcott's g factors vary with about 10^{-3} for temperature variations of 100°C the errors associated with the functions C_1, C_2 and C_3 are negligeable.

The largest errors are introduced by the experimental activity ratios, and by the uncertainties on the resonance integrals of In, Au and Mn.

The value of $(G_r \cdot s_o)_{Mn}$ had been calculated by interpolation from the data of ref.13 and is 0.8136 which means s_o=0.83, with an accuracy of 5%. The s_o of indium or gold are known within 2,5%. The error on r' is finally 5,5% for a 1% error in the activity ratio.

Since the curve of R_{Lu-Mn} against the temperature T are nearly straight lines with a slope depending on the parameter r', the error on T is given mainly by the experimental error of R_{Lu-Mn}. For a 1% error in the Lu-Mn activity ratio the error on T varies between 3 and 4 degrees depending on r'.

4.3 Discussion

For the calculation of the spectrum indices the Westcott convention was used for the points in the moderator and in the fuel. The deviation of a 1/E behaviour in the joining region

below 1 eV is taken into account utilizing the Δ_4 joining function (ref.14). This treatment is not rigorous and breaks down in the fuel because of the large thermal absorptions producing a strong hardening with a modification of the maxwellian spectrum. Although some attempts had been done to take into account the hardening effects (ref.15), these cannot be related to the neutron temperature by a simple rule. For this reasons the hardening effect was neglected and the thermal spectrum index T was calculated in the normal way. More realistic spectral models can compute the fuel activation rate ratios to be compared with the quoted values.

Acknowledgments

The author wishes to thank Mr. HAGE for the useful advices and suggestions. I am also grateful to Mr. ANSELMI and Miss DUBUJADOUX for help in counting and data processing.

Finally I would like to thank Mr. SPAEPEN and Mr. DEBUS of BCMN of Geel, Belgium for collaboration in supplying detectors.

Reference Index

1. CADILHAC, HOROWITZ, SOULE, TRETIAKOFF
Conference on neutron thermalization.
Brookhaven 1963 - BNL 719

2. C.H. Westcott et al.
Effective cross section and Cd ratios for neutron spectra of thermal reactors.
Geneva Conference 1958, Vol 16.

3. E.K. SOKOLOWSKY
Different activation techniques for the study of epithermal spectra.
AE 230.

4. BARCLAY, SANDERS
An Au-Mn activation detector for use at high temperature.
AEEW MS - 1959

5. ROBERGE, SAILOR
Nuclear Science and Engineering 7, 502-504 - 1960

6. BLAESSER, BONNAURE, CASINI, CENERINI, RAIEVSKI, TOSELLI
EUR 130 f

7. VAN AUDENHOVE, JOYEUX
Prepara-tion with levitation melting in Argon of aluminum alloy for neutron measurements.
Journal of Nuclear Materials, Vol.19, p.97 - 1966

8. ANSELMI, CONTI
Gamma chains data elaboration program.
Ispra internal report non availab-le.

9. ANL 5800

10. G.M. ROE
The absorption of neutrons in Doppler broadened resonances.
KAPL 1241

11. C. LANDES
Ispra internal report non availab le.

12. C. LANDES
Private communication.

13. F. FEINER
KAPL 2000 16

14. C.H. WESTCOTT
Effective cross section values for well moderated thermal reactor spectra.
AECL 1101

15. N.N. FOX
Characterization of thermal spectra by integral techniques.
AEEW R 342.

15. C.H. WESTCOTT
Effective fission and capture cross sections for hardened maxwellian neutron spectra.
Reactor Science 1960, Vol.12,p. 113

Fig. 1 - GEOMETRY OF THE 4-UC-30.9 FUEL ELEMENT

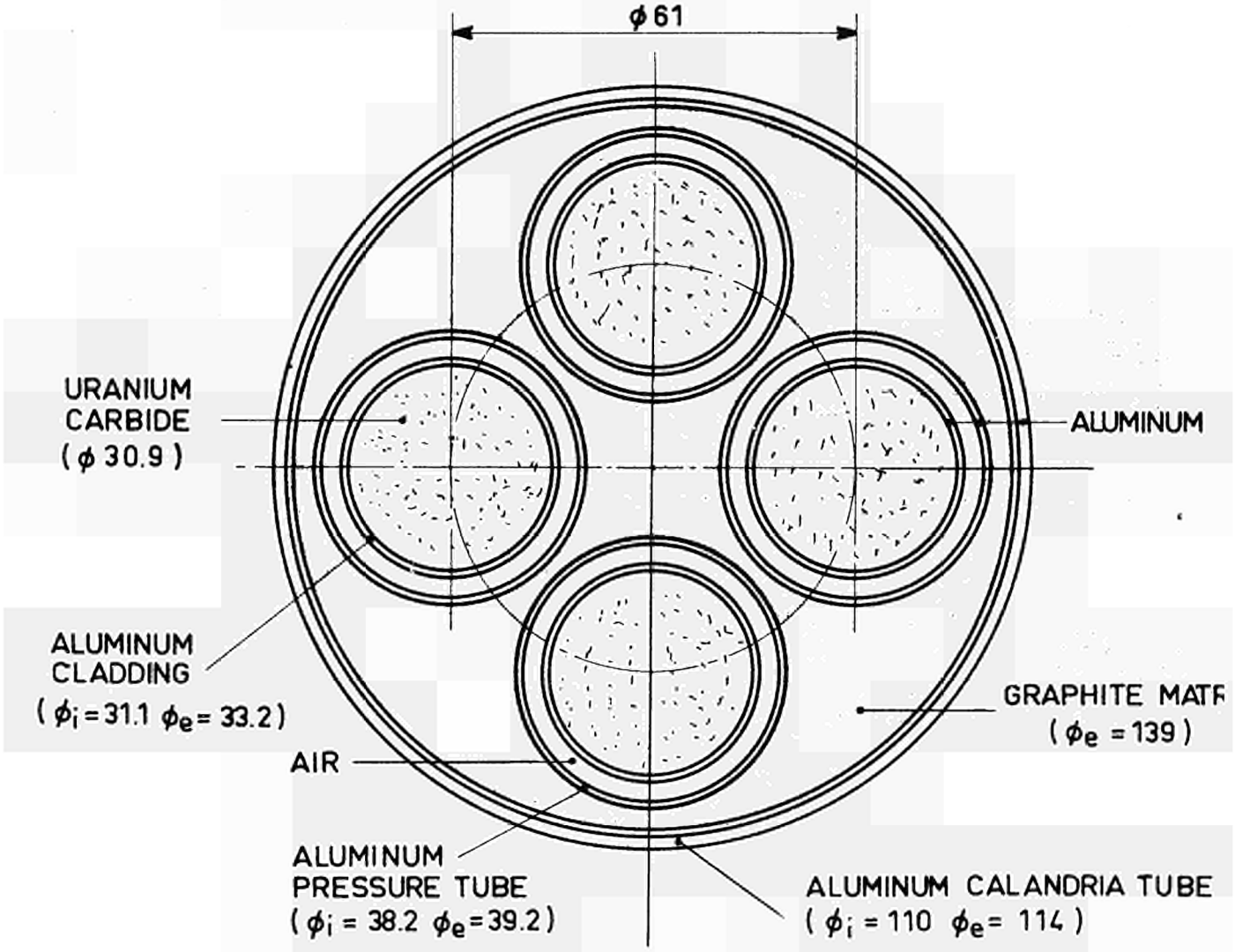

Dimensions in mm.

FIG. 2. GEOMETRY OF UC/7/25.2 FUEL ELEMENT

FUEL CLUSTER CROSS SECTION VIEW

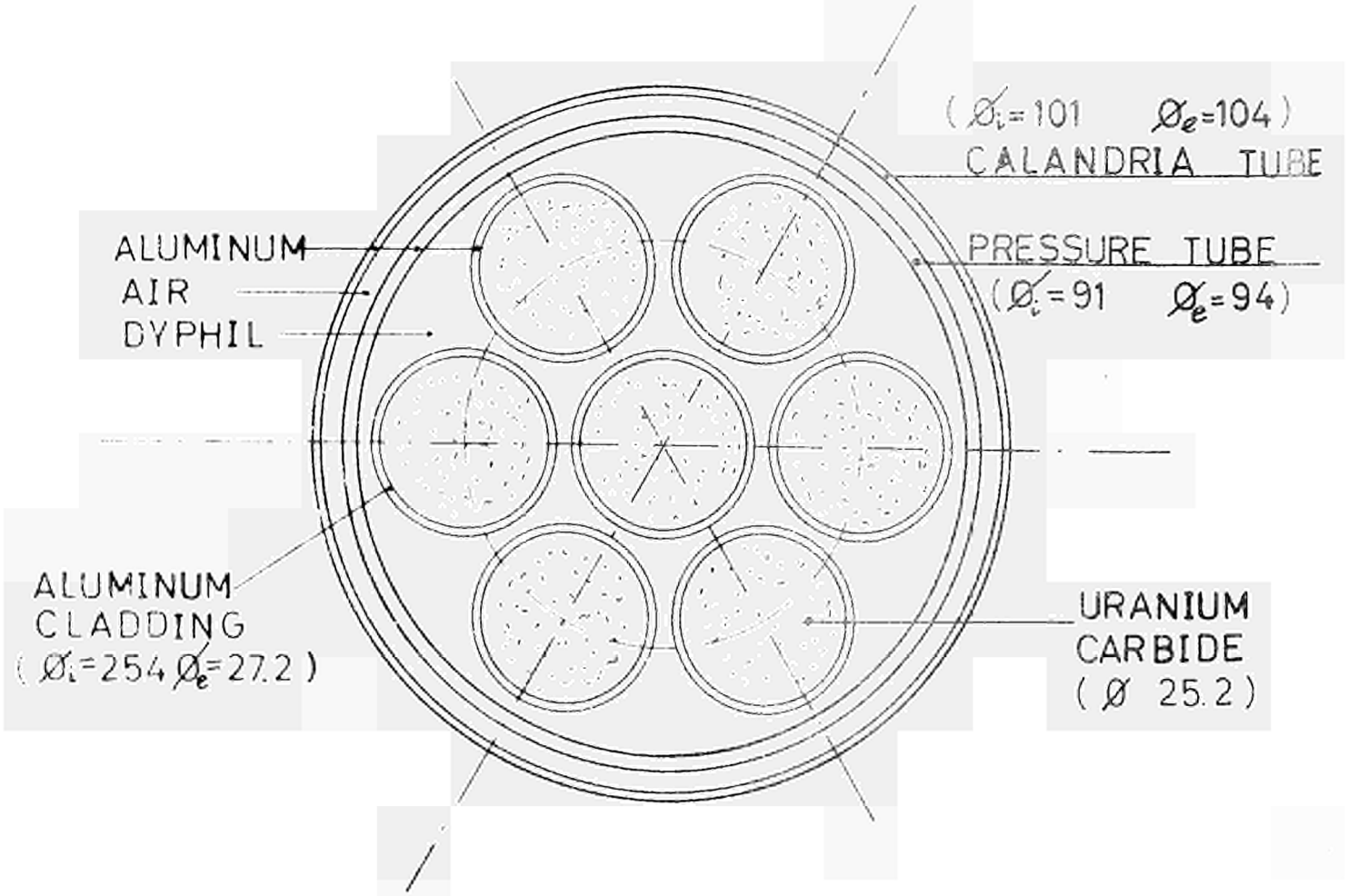

Dimensions in mm

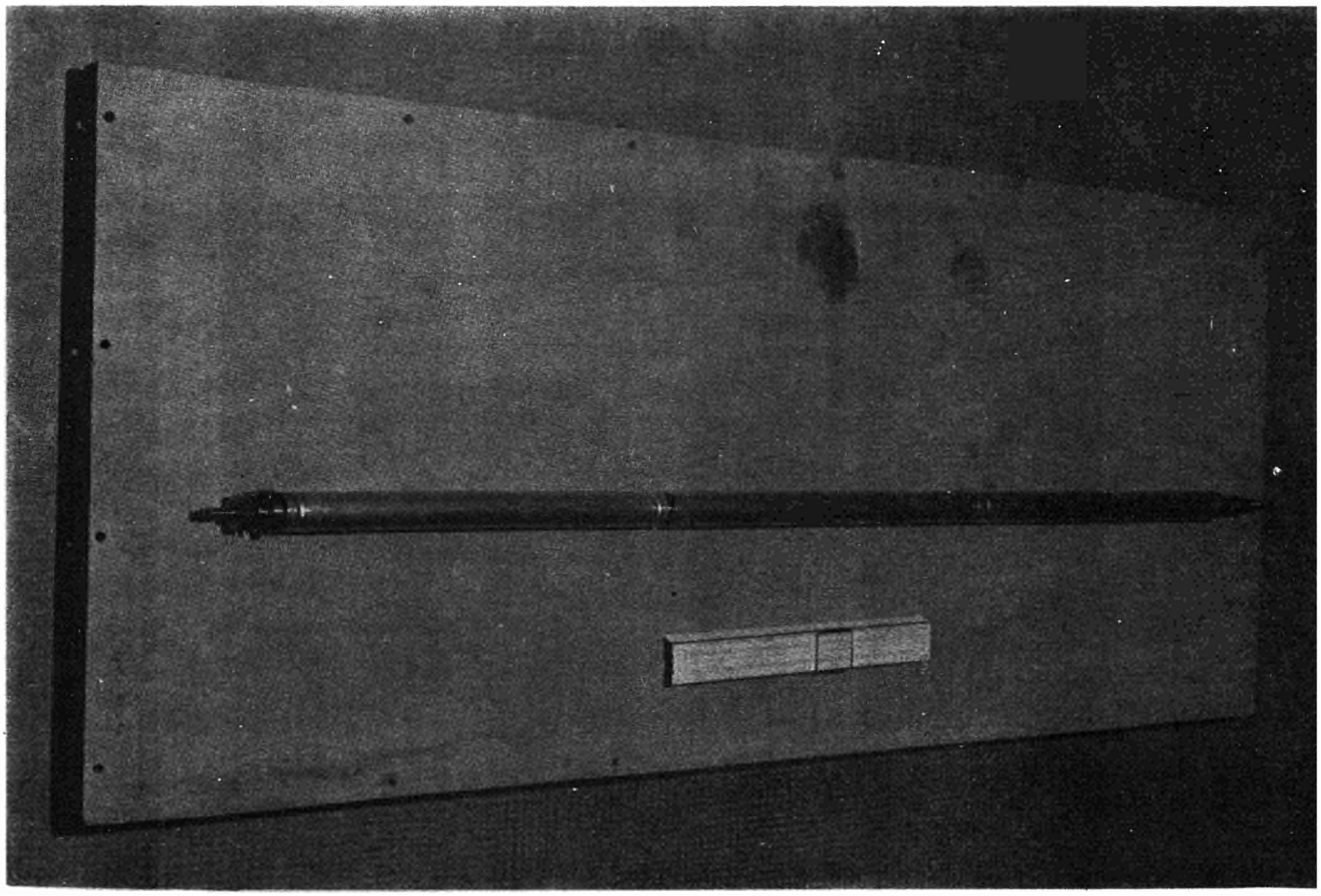

Fig. 3 Special measuring rod

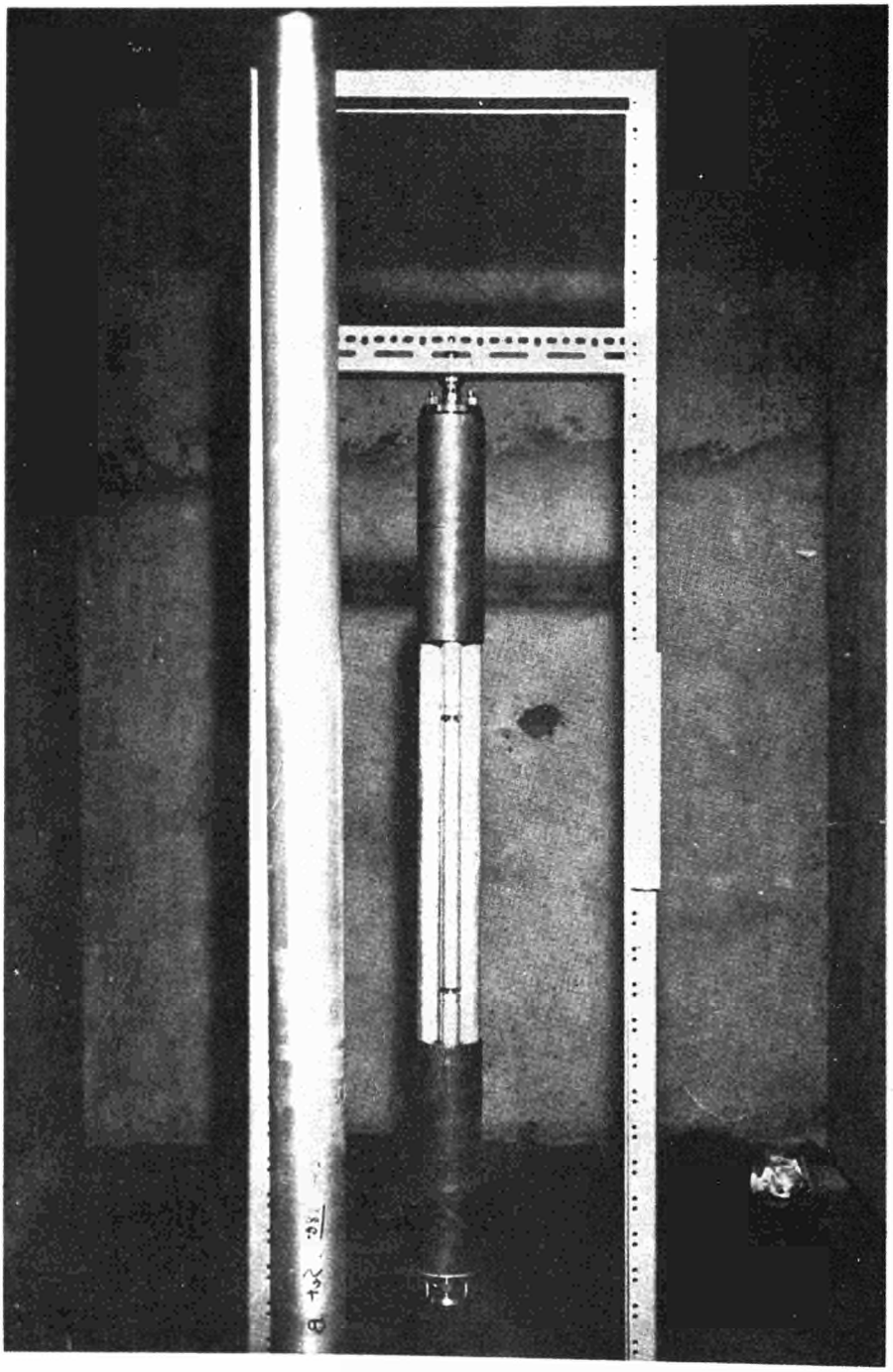

Figure 4
Special fuel element
view during the assemblig

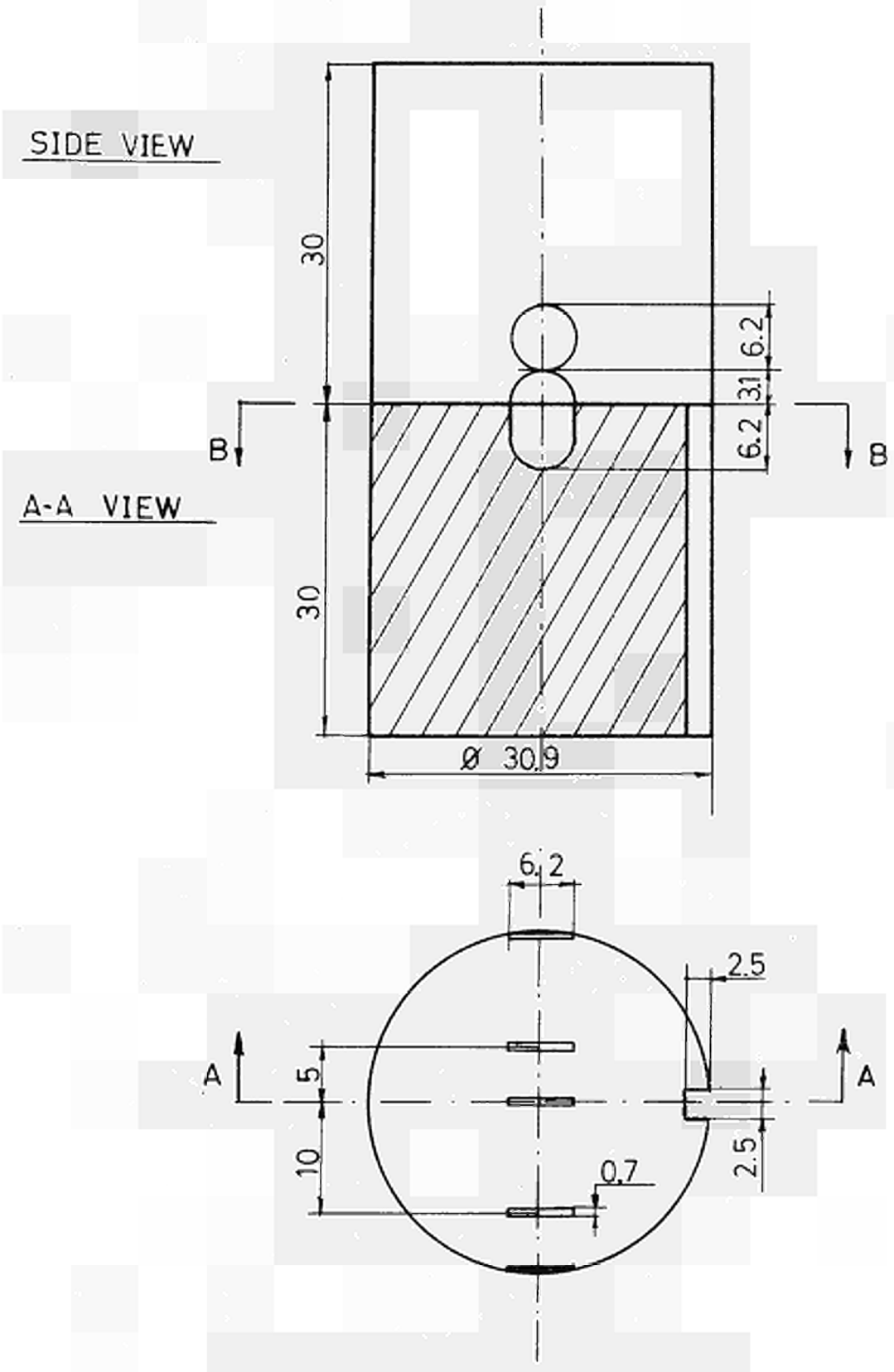

SPECIAL UC PELLET WITH
HOLES FOR 6.0 MM DETECTORS

FIG. 5

Fig. 6 DETECTOR ARRANGEMENT

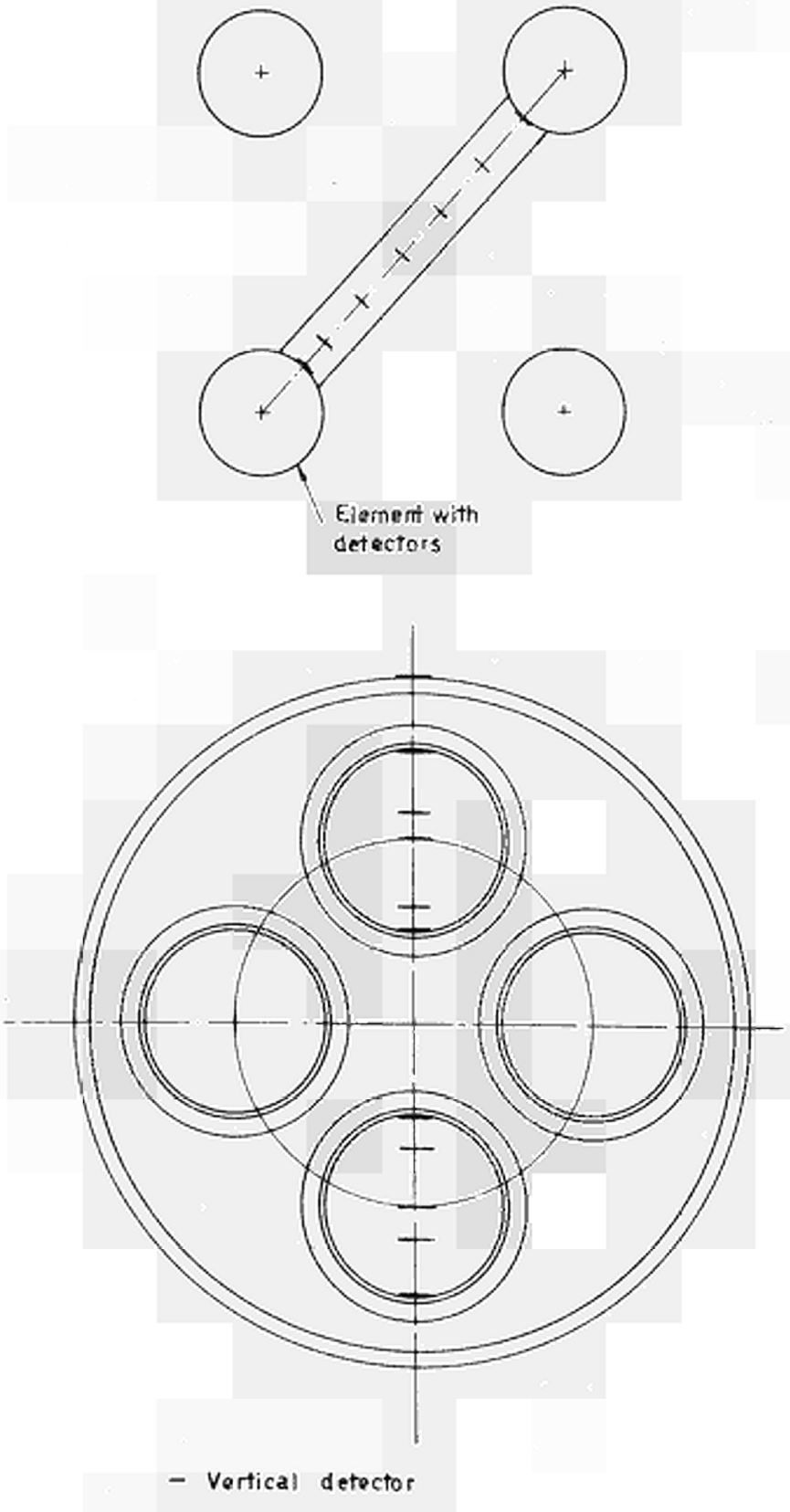

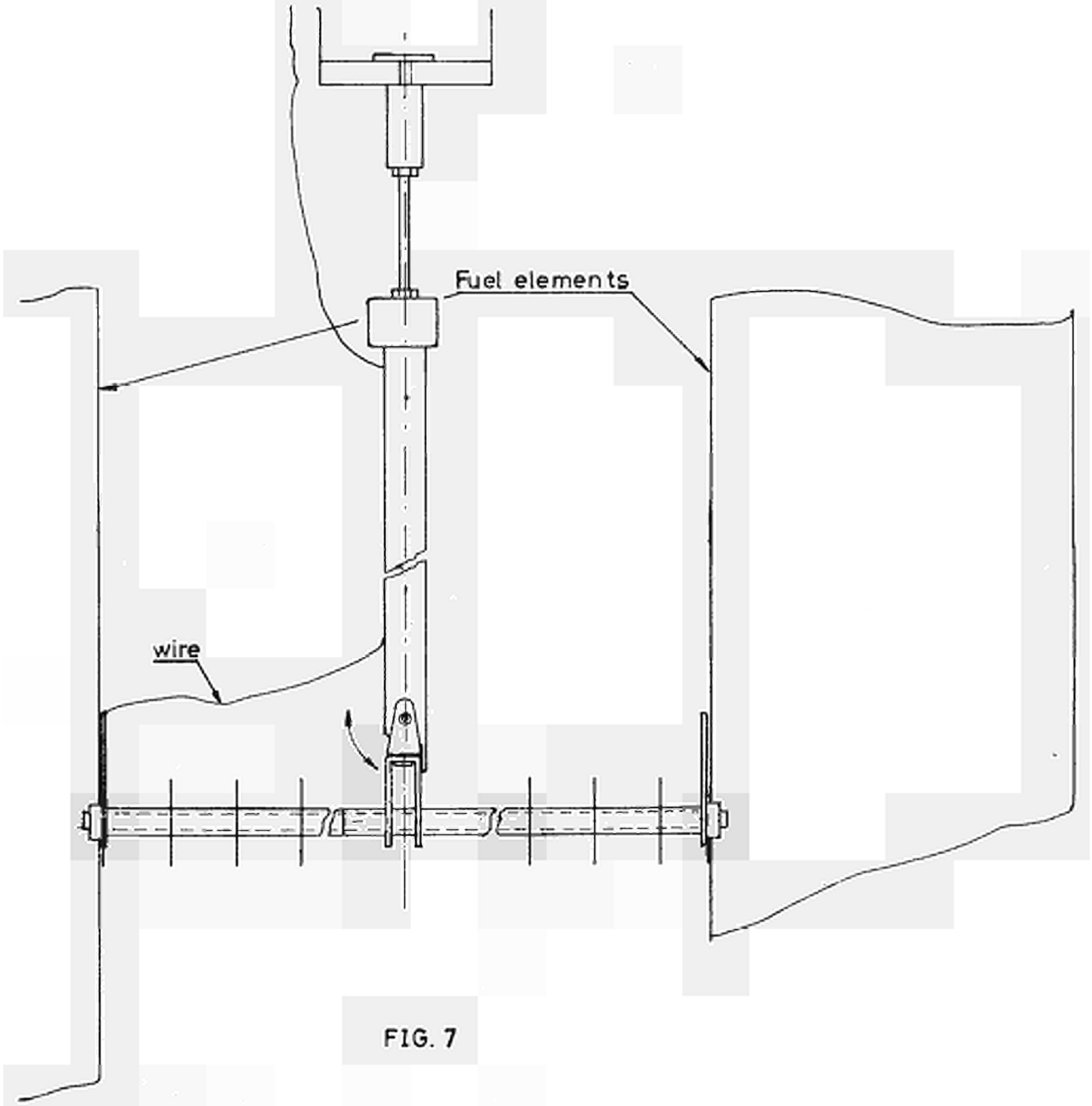

FIG. 7

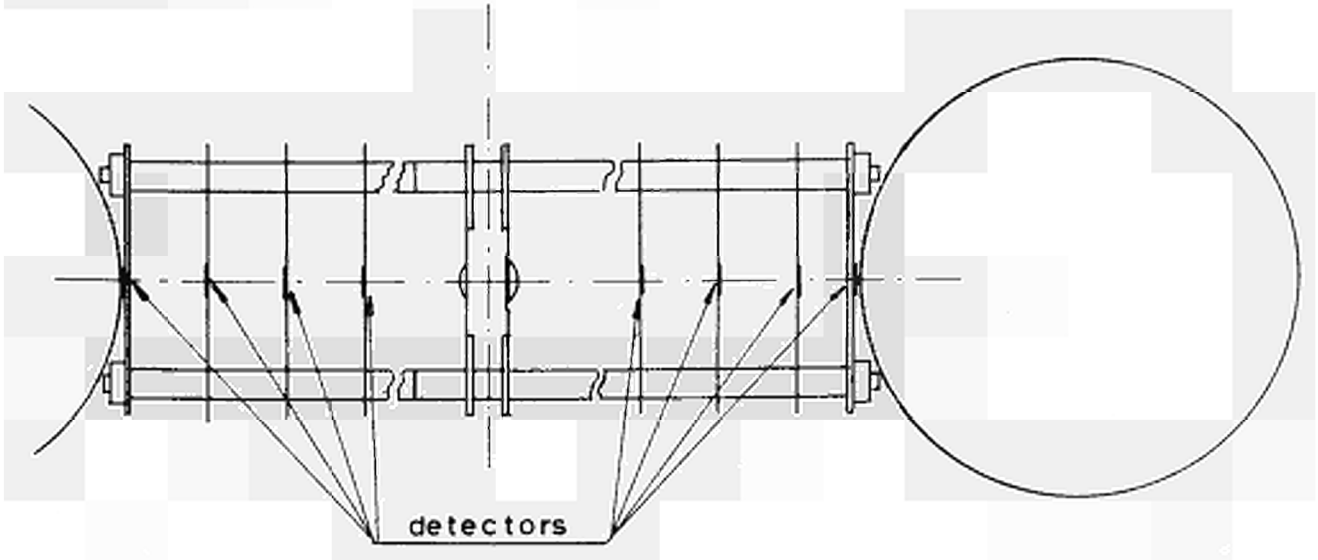

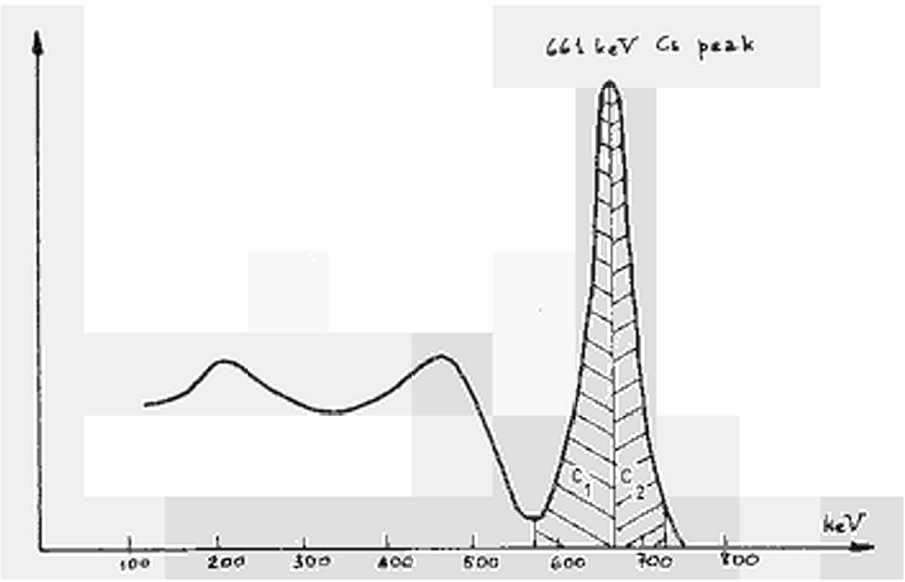
661 keV Cs peak
C1
C2
keV
100
200
300
400
500
600
700
800

FIG. 8

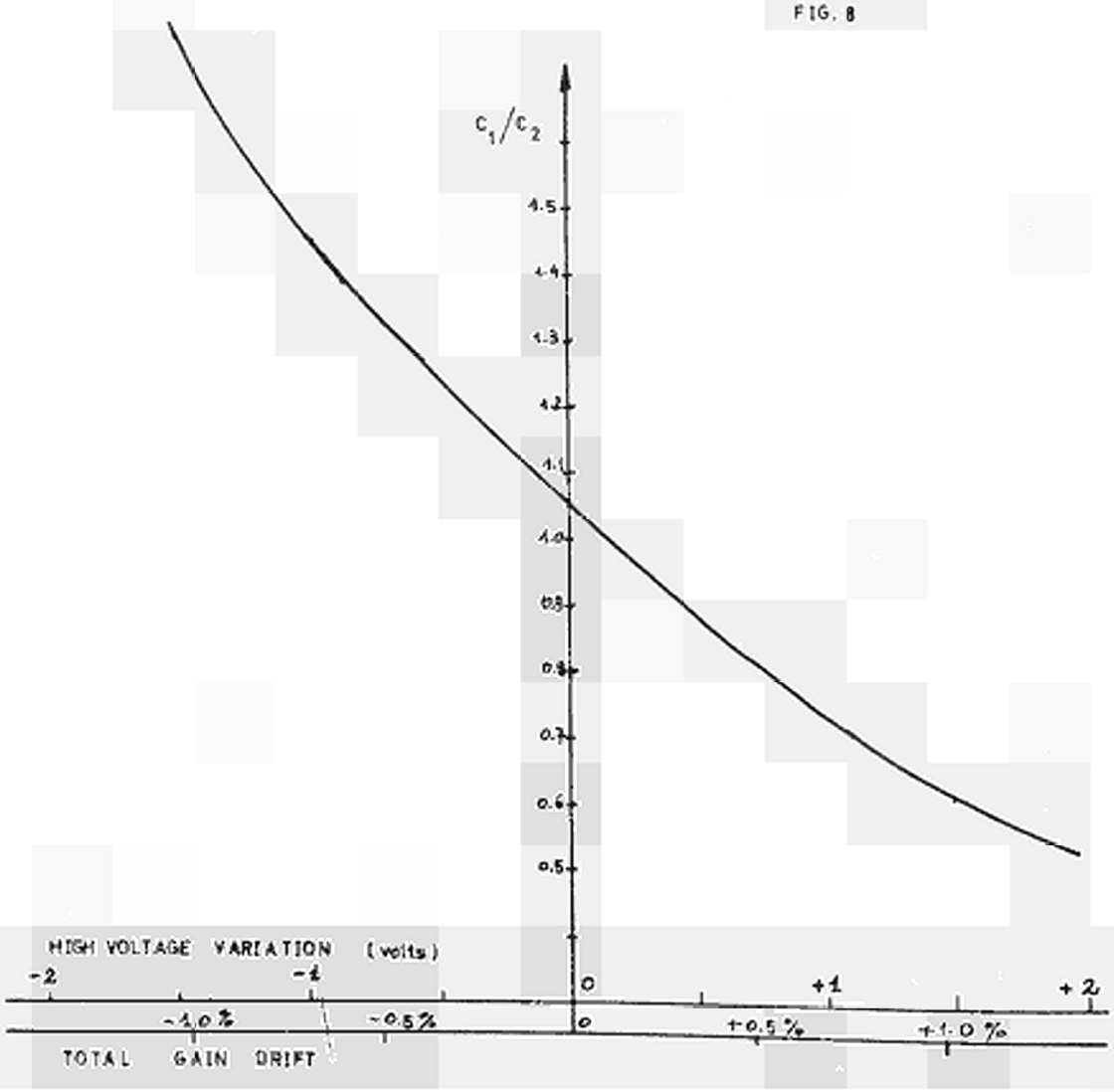
C1/C2
1.5
1.4
1.3
1.2
1.1
1.0
0.9
0.8
0.7
0.6
0.5
HIGH VOLTAGE VARIATION (volts)
-2
-1
0
+1
+2
-1.0 %
-0.5 %
0
+0.5 %
+1.0 %
TOTAL GAIN DRIFT

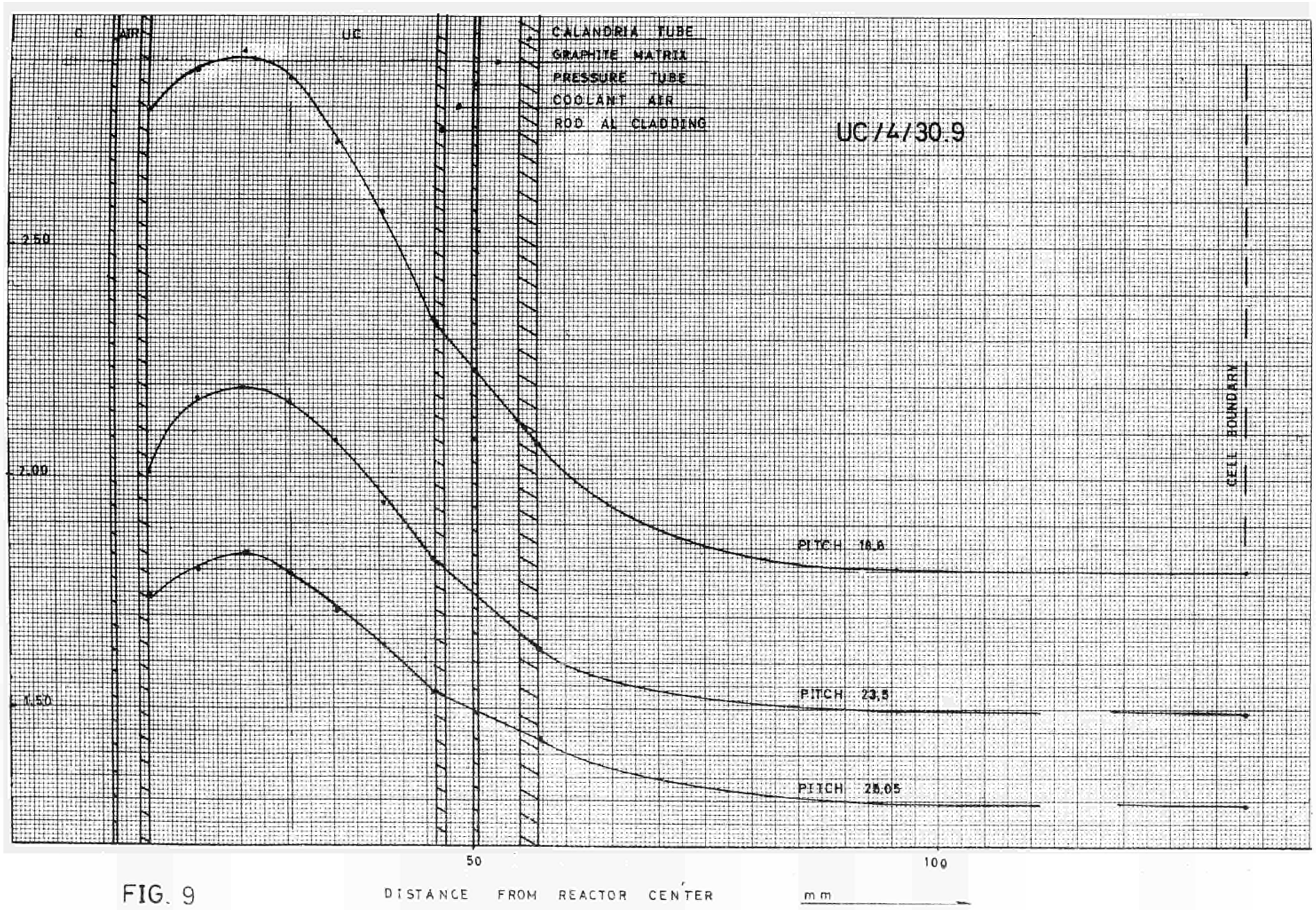
C
AIR
UC
CALANDRIA TUBE
GRAPHITE MATRIX
PRESSURE TUBE
COOLANT AIR
ROD AL CLADDING
UC/4/30.9
2.50
2.00
1.50
PITCH 18.8
PITCH 23.5
PITCH 25.05
CELL BOUNDARY
50
100
mm
DISTANCE FROM REACTOR CENTER
R IN-MN IN-MN ACTIVITY RATIOS

FIG. 9

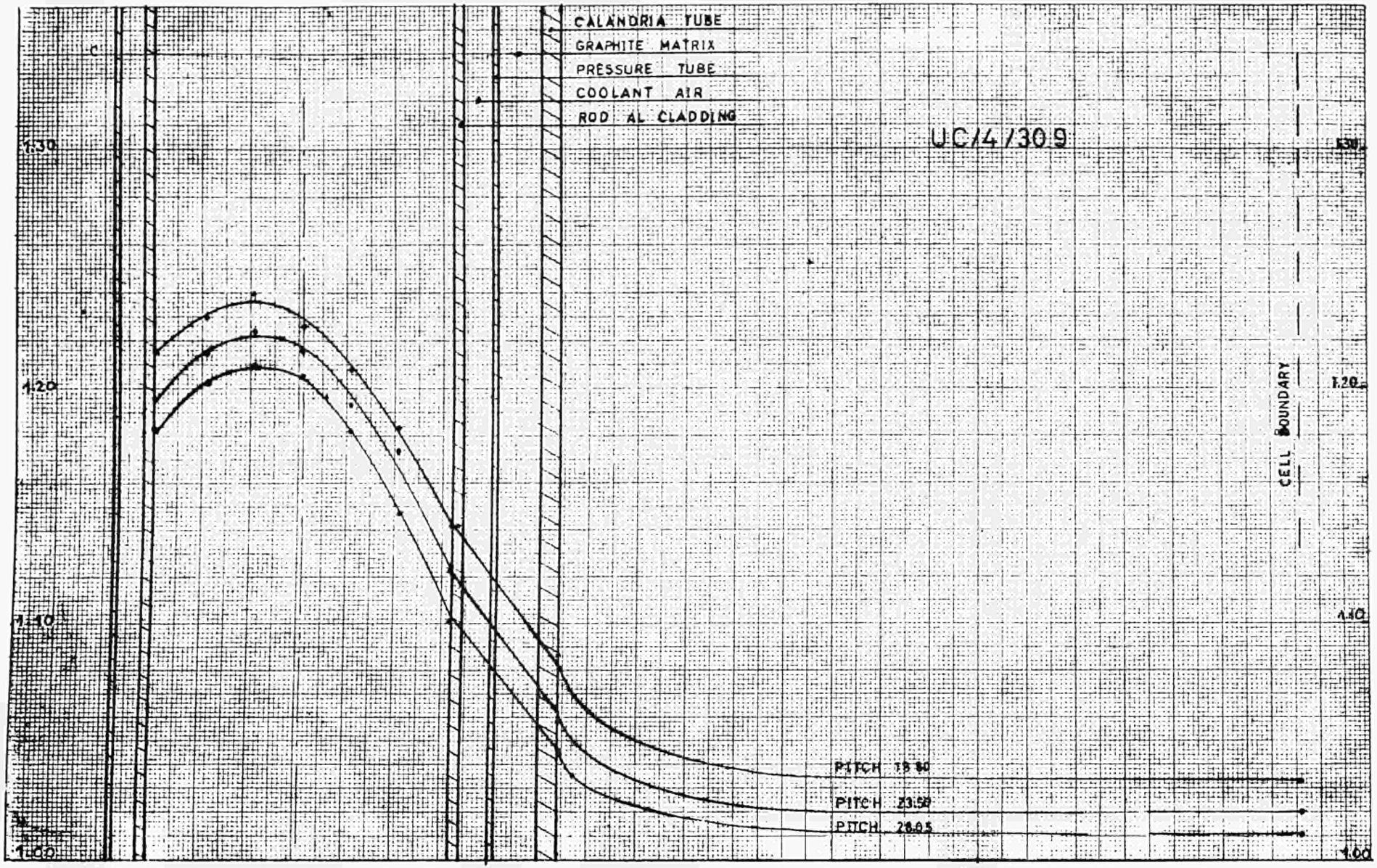
CALANDRIA TUBE
GRAPHITE MATRIX
PRESSURE TUBE
COOLANT AIR
ROD AL CLADDING
UC/4/309
CELL BOUNDARY
PITCH 18.80
PITCH 23.50
PITCH 28.05
1.30
1.20
1.10
1.00
50
100
mm
DISTANCE FROM REACTOR CENTER
R LU-MN
LU-MN ACTIVIT. RATIOS

FIG. 10

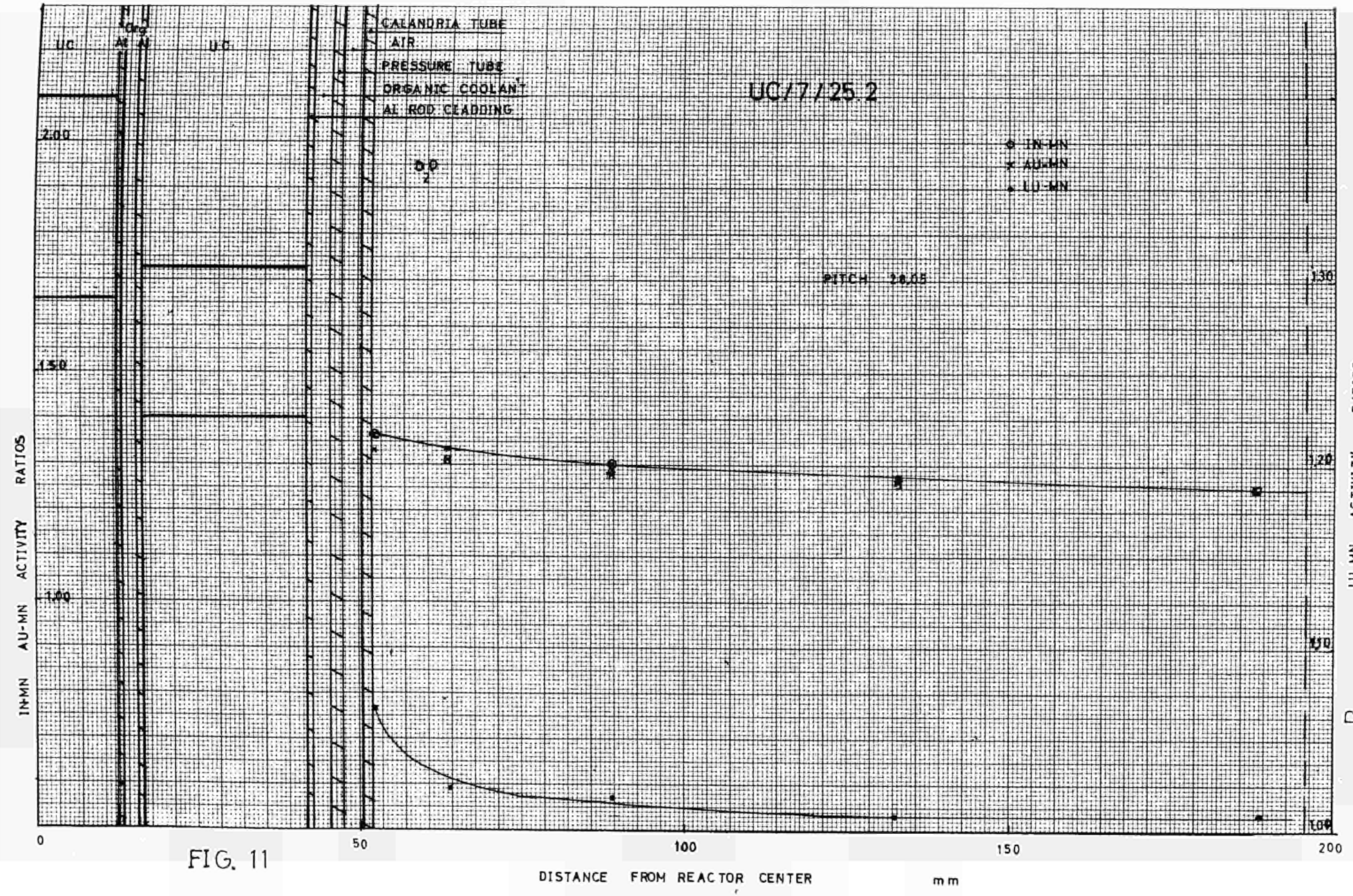
UC
Al
Al
UC
CALANDRIA TUBE
AIR
PRESSURE TUBE
ORGANIC COOLANT
AL ROD CLADDING
UC/7/25.2
IN-MN
AU-MN
LU-MN
PITCH 28.05
2.00
1.50
1.00
1.30
1.20
1.10
1.00
IN-MN AU-MN ACTIVITY RATIOS
LU MN ACTIVITY RATIOS
R_{LU-MN}
0
50
100
150
200
DISTANCE FROM REACTOR CENTER
mm

FIG. 11

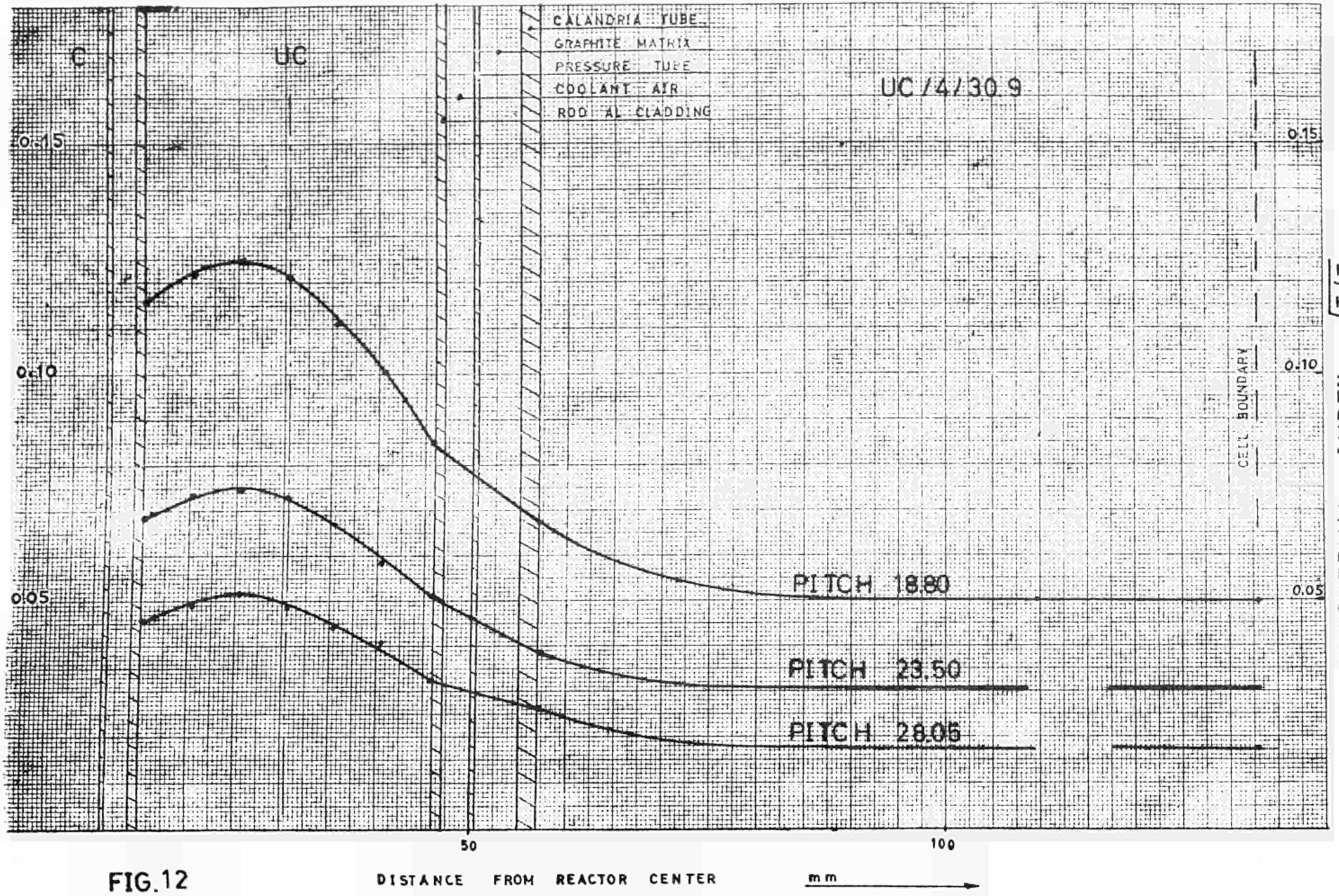
C
UC
CALANDRIA TUBE
GRAPHITE MATRIX
PRESSURE TUBE
COOLANT AIR
ROD AL CLADDING
UC/4/30.9
0.15
0.10
0.05
CELL BOUNDARY
PITCH 18.80
PITCH 23.50
PITCH 28.05
50
100
DISTANCE FROM REACTOR CENTER
mm
EPITHERMAL INDEX $r\sqrt{T/T_o}$

FIG.12

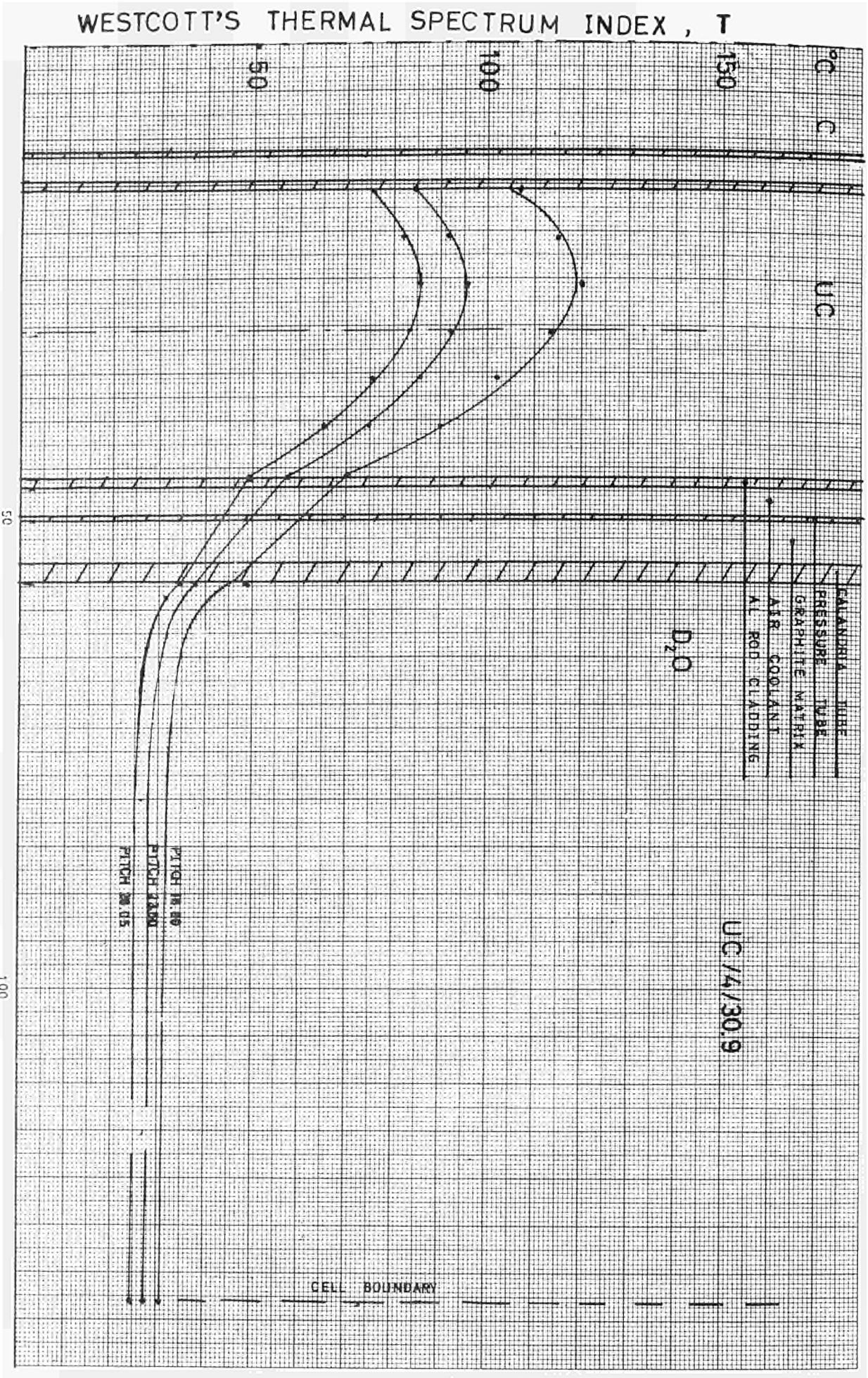
WESTCOTT'S THERMAL SPECTRUM INDEX , T
50
100
150
°C
UC
D2O
UC/4/30.9
CALANDRIA TUBE
PRESSURE TUBE
GRAPHITE MATRIX
AIR COOLANT
AL ROD CLADDING
PITCH 18.80
PITCH 23.00
PITCH 28.05
CELL BOUNDARY
50
100
DISTANCE FROM REACTOR CENTER (mm)

FIG. 13

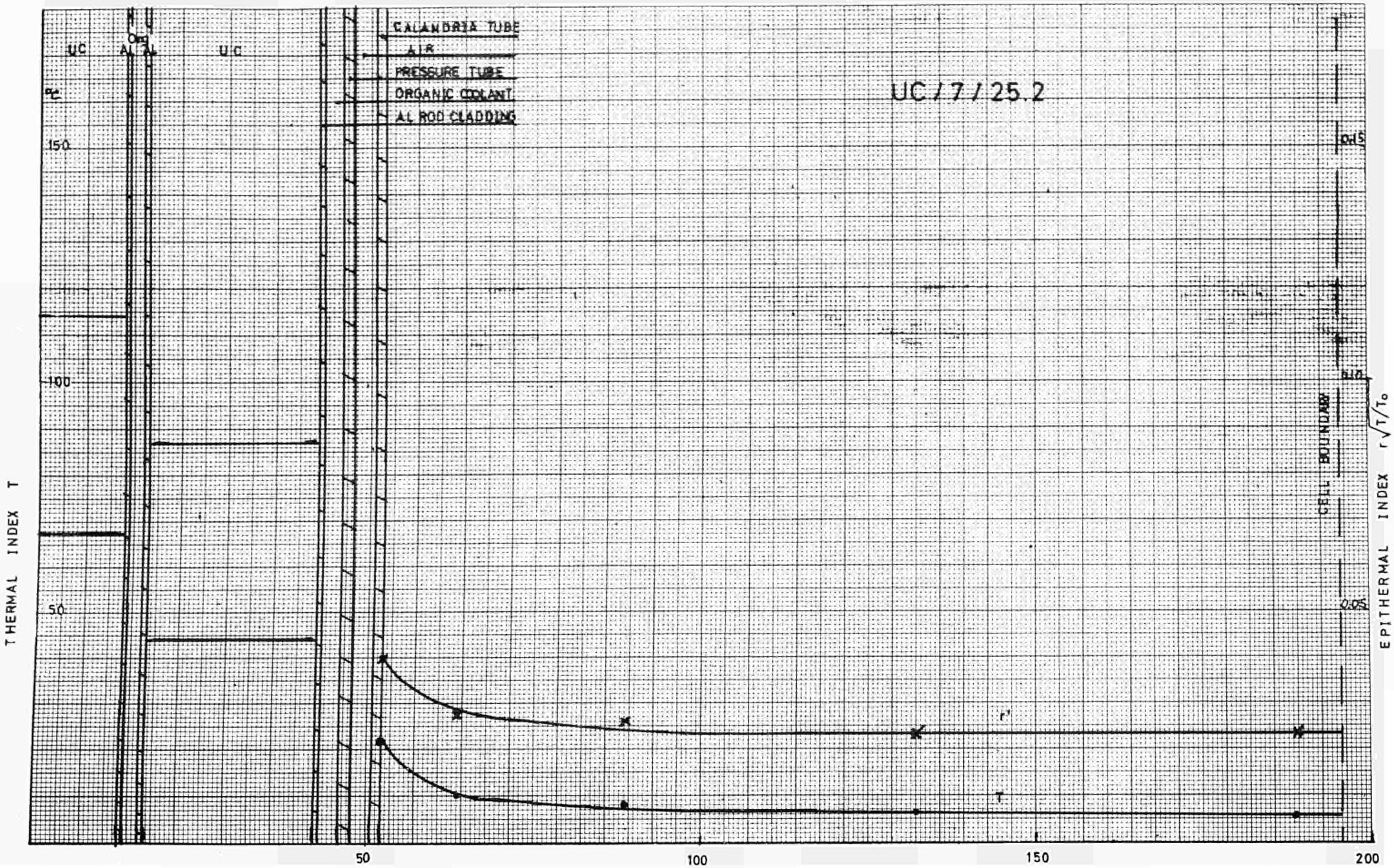
UC/7/25.2
UC
Org
Al
UC
CALANDRIA TUBE
AIR
PRESSURE TUBE
ORGANIC COOLANT
Al ROD CLADDING
°C
150
100
50
THERMAL INDEX T
CELL BOUNDARY
0.5
EPITHERMAL INDEX $r\sqrt{T/T_0}$
r'
T
50
100
150
200
DISTANCE FROM CORE CENTER (mm)

FIG 14

UC/4/30.9
radius
(mm)
+25.5 Rod max value
⊡46.0 Rod outest point
⊕57.0 Calandria tube
▲ Cell boundary
WESTCOTT'S EPITHERMAL INDEX r
0.15
0.10
0.05
20
25
30
LATTICE PITCH (cm)

FIG. 15

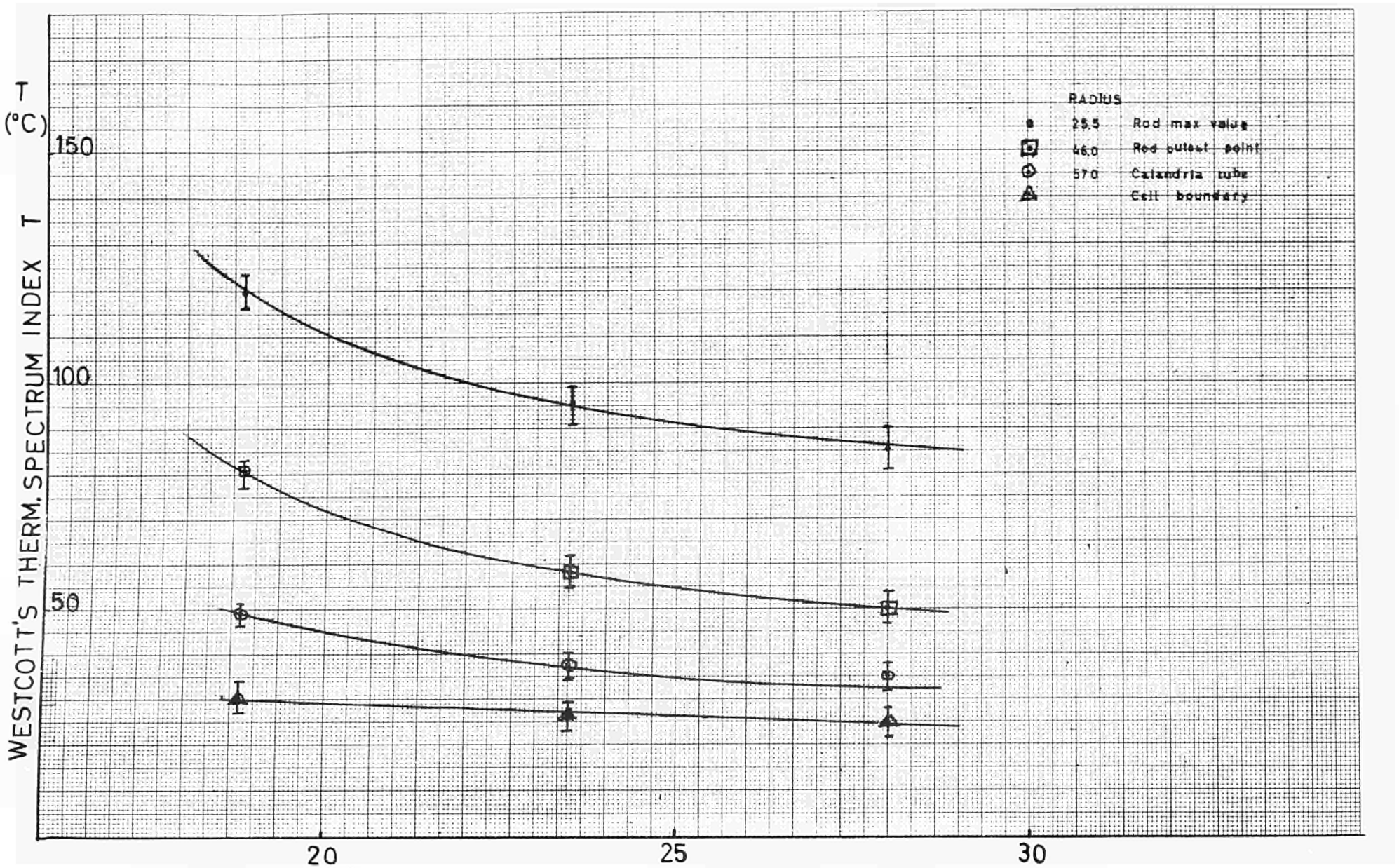
T
(°C)
150
100
50
WESTCOTT'S THERM. SPECTRUM INDEX T
RADIUS
25.5 Rod max value
46.0 Rod outlet point
57.0 Calandria tube
Cell boundary
20
25
30
LATTICE PITCH (cm)

FIG. 16

NOTICE TO THE READER

All Euratom reports are announced, as and when they are issued, in the monthly periodical **EURATOM INFORMATION,** edited by the Centre for Information and Documentation (CID). For subscription (1 year : US$ 15, £ 5.7) or free specimen copies please write to :

Handelsblatt GmbH
"Euratom Information"
Postfach 1102
D-4 Düsseldorf (Germany)

or

Office de vente des publications
des Communautés européennes
2, Place de Metz
Luxembourg

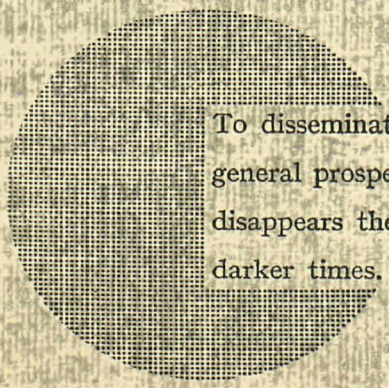

To disseminate knowledge is to disseminate prosperity — I mean general prosperity and not individual riches — and with prosperity disappears the greater part of the evil which is our heritage from darker times.

Alfred Nobel

SALES OFFICES

All Euratom reports are on sale at the offices listed below, at the prices given on the back of the front cover (when ordering, specify clearly the EUR number and the title of the report, which are shown on the front cover).

OFFICE CENTRAL DE VENTE DES PUBLICATIONS DES COMMUNAUTES EUROPEENNES
2, place de Metz, Luxembourg (Compte chèque postal Nº 191-90)

BELGIQUE — BELGIË
MONITEUR BELGE
40-42, rue de Louvain - Bruxelles
BELGISCH STAATSBLAD
Leuvenseweg 40-42, - Brussel

DEUTSCHLAND
BUNDESANZEIGER
Postfach - Köln 1

FRANCE
SERVICE DE VENTE EN FRANCE DES PUBLICATIONS DES COMMUNAUTES EUROPEENNES
26, rue Desaix - Paris 15e

ITALIA
LIBRERIA DELLO STATO
Piazza G. Verdi, 10 - Roma

LUXEMBOURG
OFFICE CENTRAL DE VENTE DES PUBLICATIONS DES COMMUNAUTES EUROPEENNES
9, rue Goethe - Luxembourg

NEDERLAND
STAATSDRUKKERIJ
Christoffel Plantijnstraat - Den Haag

UNITED KINGDOM
H. M. STATIONERY OFFICE
P. O. Box 569 - London S.E.1

EURATOM — C.I.D.
51-53, rue Belliard
Bruxelles (Belgique)